

2012

Direct measurements and numerical simulations of gas charging in microelectromechanical system capacitive switches

A Venkatraman

A Garg

D Peroulis

Alina A. Alexeenko

Purdue University - Main Campus, alexeenk@purdue.edu

Follow this and additional works at: <http://docs.lib.purdue.edu/aaepubs>



Part of the [Engineering Commons](#)

Recommended Citation

Venkatraman, A; Garg, A; Peroulis, D; and Alexeenko, Alina A., "Direct measurements and numerical simulations of gas charging in microelectromechanical system capacitive switches" (2012). *School of Aeronautics and Astronautics Faculty Publications*. Paper 36.
<http://dx.doi.org/10.1063/1.3688176>

This document has been made available through Purdue e-Pubs, a service of the Purdue University Libraries. Please contact epubs@purdue.edu for additional information.

Direct measurements and numerical simulations of gas charging in microelectromechanical system capacitive switches

A. Venkatraman,¹ A. Garg,^{2,3} D. Peroulis,^{2,3} and A. A. Alexeenko^{1,3,a)}

¹*School of Aeronautics and Astronautics, Purdue University, West Lafayette, Indiana 47907, USA*

²*School of Electrical and Computer Engineering, Purdue University, West Lafayette, Indiana 47907, USA*

³*Birk Nanotechnology Center, Purdue University, West Lafayette, Indiana 47907, USA*

(Received 29 October 2011; accepted 5 February 2012; published online 22 February 2012)

Gas breakdown in microelectromechanical system capacitive switches is demonstrated using high resolution current measurements and by particle-in-cell/Monte Carlo collision (PIC/MCC) simulations. Measurements show an electric current through a 3 μm air gap increasing exponentially with voltage, starting at 60 V. PIC/MCC simulations with Fowler-Nordheim [Proc. R. Soc. London, Ser. A **119**, 173 (1928)] field emission reveal self-sustained discharges with significant ion enhancement and a positive space charge. The effective ion-enhanced field emission coefficient increases with voltage up to about 0.3 with an electron avalanche occurring at 159 V. The measurements and simulations demonstrate a charging mechanism for microswitches consistent with earlier observations of gas pressure and composition effects on lifetime. © 2012 American Institute of Physics. [doi:10.1063/1.3688176]

Radio frequency (RF) microelectromechanical system (MEMS) capacitive switch technology has significant advantages¹ including low loss, high isolation, high linearity, and bandwidth at a very low power consumption. However, improved knowledge of ageing mechanisms and physics of failure of RF MEMS is necessary for development of reliable designs of these systems. The most commonly observed failure mode in capacitive RF MEMS switches is permanent stiction of the metal bridge to the solid dielectric. The major underlying reason for stiction between clean surfaces is believed to be related to charge trapping in the solid dielectric, which is referred to as dielectric charging.^{1–3} The charge is injected to the dielectric during contact with the metallic bridge at each switching cycle. Though gas in the gap between the bridge and the solid dielectric presents another charging medium, gas electrostatic breakdown was considered improbable since actuation voltages in capacitive switches are typically much lower (<100 V) than the minimum breakdown voltage predicted by the classical Paschen law given by⁴

$$V_b = \frac{B_p p d}{\log(A_p p d) - \log(\log(1 + 1/\gamma_{se}))}, \quad (1)$$

where A_p and B_p are constants depending on the gas, and γ_{se} is the secondary electron emission coefficient. The Paschen law predicts a minimum breakdown voltage of about 330 V for atmospheric pressure air, occurring for a gap size of about 10 μm . Past experiments, summarized by Go and Pohlman,⁵ have observed glows, sparks, and other charging phenomena in microgaps of various gases at voltages much lower than that given by the Paschen law. For example, Torres and Dhariwal⁶ performed experiments to characterize breakdown in air for gap sizes varying from 500 nm to 25 μm and obtained an almost linear drop in breakdown volt-

age for gap sizes between 4 μm and 500 nm and attributed this to field emission of electrons from the cathode. In the presence of an ambient gas, emitted electrons may ionize neutral molecules leading to production of ions which in turn modify the cathode electric field and enhance the cathode emission. This results in a self-sustained microdischarge. In order to describe gas breakdown for all gap sizes, the Paschen law has been modified to include the effects of field emission in microgaps. The *modified Paschen law*⁷ predicts nearly linear increase in breakdown voltage at very small gaps followed by a transition to the macroscale Paschen law. Experimental evidences consistent with gas breakdown have also been observed in electrostatic MEMS devices with lifetime of these showing a strong dependence on gas pressure⁸ and gas composition.^{9,10}

The main goal of this work is to study the onset of breakdown and probe the structure of microscale gas discharges in MEMS capacitive switches using direct measurements of current vs voltage and numerical simulations. Specifically, numerical simulations are used to quantify key parameters such as net charge and ion-enhancement field emission coefficient as a function of voltage. The remainder of the letter is organized as follows: first, we briefly describe the theory of gas breakdown in microgaps including the process of field emission and a general form of the mathematical model for the modified Paschen law. Then, measurement and simulation results are presented and discussed.

The process of field emission is described by the Fowler-Nordheim (F-N) theory¹¹ which gives a relation between the current density of emitted electrons and the electric field as

$$j_{\text{FN}} = \frac{A_{\text{FN}} \beta^2 E^2}{\phi t^2(y)} \exp\left(-\frac{B_{\text{FN}} \phi^{3/2} v(y)}{\beta E}\right), \quad (2)$$

where j_{FN} is the current density, E is the electric field intensity, ϕ is the work function of the cathode material, β is the

^{a)}Author to whom correspondence should be addressed. Electronic mail: alexeenk@ecn.purdue.edu.

field enhancement factor, and $A_{FN} = 6.2 \times 10^{-6} \text{ A/eV}$ and $B_{FN} = 6.85 \times 10^7 \text{ V/cm/eV}^{3/2}$ are Fowler-Nordheim constants. Barrier shape functions $v(y) \approx 0.95 - y^2$ and $t^2(y) \approx 1.1$ with $y \approx 3.79 \times 10^{-4} \sqrt{\beta E}/\phi$ were not part of the original Fowler-Nordheim equation and were corrections included later.¹²

The field enhancement factor, β , is a strong function of the surface roughness which makes it hard to predict. Values of β ranging from 1.5 to 115 have been reported in various experiments in the past¹³ for atomically rough surfaces.

Recently, two mathematical models^{5,14} for the modified Paschen law have been presented. The general form of both models is given by

$$(\gamma_{se} + \gamma') [e^{A_p p d \exp(-B_p p d / V_b)} - 1] = 1. \quad (3)$$

It should be noted that the above equation is similar to the Townsend criterion⁴ for breakdown but includes the effects of ion-enhanced field emission through the second term γ' . While the first model⁵ uses a fitting parameter K , the second model¹⁴ has no uncertain parameters but makes assumptions with regard to the location of ion creation and mobility. In this work, instead of approximate theoretical considerations, we use numerical simulations to obtain estimates of γ' and its dependence on applied voltage for a $3 \mu\text{m}$ nitrogen gap corresponding to experimental setup described below.

High resolution current vs voltage measurements were performed at Purdue University for typical MEMS switch structures with a nominal air gap of $3 \mu\text{m}$ at atmospheric pressure. The experimental setup is described in detail by Garg *et al.*¹⁵ Figure 1 (top) shows a micrograph of a typical MEMS structure with an electrode overlap area of $120 \mu\text{m} \times 270 \mu\text{m}$ and a thickly plated Ni bridge to avoid deflection for voltages less than a few kV. Figure 1 (bottom) shows measured current as a function of voltage for two typical devices and the corresponding F-N theory for various values of field enhancement factor, β . In obtaining the F-N theory curves, it was assumed that the field emission is due to surface roughness that is uniformly distributed on the cathode surface and the value of $\phi = 5.15$ corresponding to a nickel cathode was used. The exponential increase in current as a function of voltage, starting at about 60 V, indicates field emission from the cathode as the main gas discharge mechanism.

In order to determine the microdischarge structure and quantify the contribution of ion-enhanced field emission rigorously, particle-in-cell/Monte Carlo collision (PIC/MCC) simulations were performed. A one-dimensional code XPDP1 (Ref. 16) was used to obtain the microdischarge structures including ion and electron number densities and current densities. The simulations were performed for N_2 gas at atmospheric pressure and for a gap of $3 \mu\text{m}$. The XPDP1 code was modified by including a flux of electrons at the cathode based on the F-N theory current density and the local computed electric field. Five collision mechanisms have been considered including three electron-neutral collisions, i.e., elastic scattering, excitation, ionization to N_2^+ , and two ion-neutral collisions, i.e., elastic scattering and charge exchange. The simulations used a value of $\beta = 55$ as extracted from measurements in this work. The value of $\gamma_{se} = 0.05$ was chosen based on previous work.¹⁷

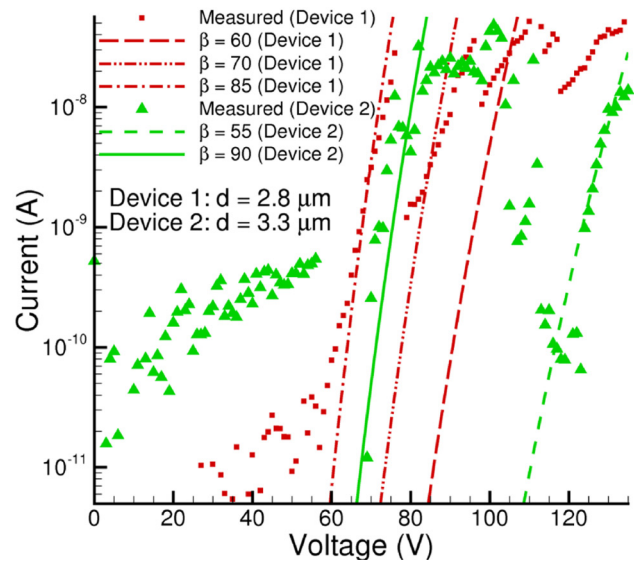
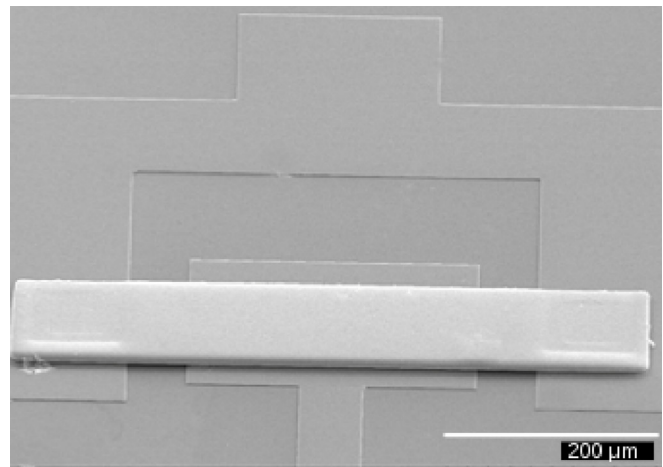


FIG. 1. (Color online) (top) SEM of a typical MEMS structure and (bottom) I-V curves obtained from measurements for typical MEMS structures compared with the F-N theory for various values of field enhancement factor β . The gap for device 1 was $2.8 \mu\text{m}$ and the gap for device 2 was $3.3 \mu\text{m}$.

Figure 2 shows the computed steady state ion and electron number density profiles in the gap. Here, $X = 0$ and $X = 3 \mu\text{m}$ represent the anode and cathode, respectively. For a given value of the applied voltage, the ion number density increases from the anode to the cathode. Also, due to disparity in drift velocities, the electron number density is more than two orders of magnitude lower than the ion number density thereby resulting in a net positive charge in the gap. The variation of ion number density from anode to cathode is more pronounced than the corresponding electron number density variation. The obtained positively charged discharge can be classified as a Townsend dark discharge.⁴

Figure 3 shows the variation of ion and electron current density in the gap at 153 V and 155 V. It can be seen that the electron carries all the current at the anode while the cathode current is shared by both ions and electrons. A summary of various discharge parameters is presented in Table I showing that the positive charge in the gap increases rapidly with increasing voltage. Due to ionization, the actual current density in the gap is greater than the value using F-N theory with the nominal electric field (V/d). The ratio $j_{\text{actual}}/j_{FN} = 1$ in the absence of ionization (in very small gaps much smaller

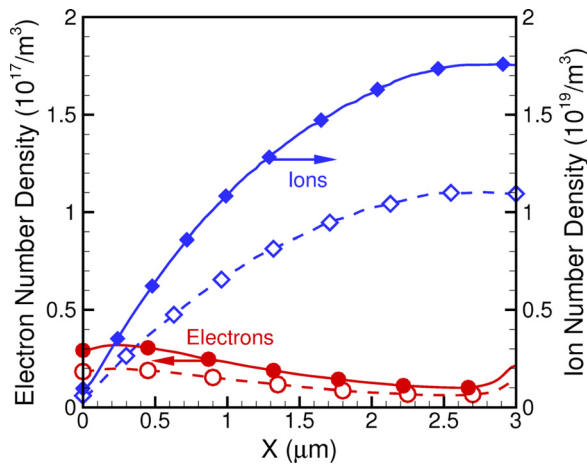


FIG. 2. (Color online) Comparison of ion and electron number density profiles across the $3\ \mu\text{m}$ nitrogen gap for an applied voltage of 153 V and 155 V. The solid lines with filled symbols correspond to 155 V and the dashed lines with open symbols correspond to 153 V. The diamond symbols correspond to ions and the circles correspond to electrons.

than the mean free path or in vacuum) and all the current is carried by the electrons with no ion-enhancement. For voltages of 90 V and 120 V, the positive charge in the gap is not significant enough to modify the electric field from its nominal value of V/d . Therefore, the ratio $j_{\text{actual}}/j_{FN} > 1$ is completely due to ionization in the gap. On the other hand, at higher voltages, the larger positive charge also leads to a modification of the cathode electric field thereby increasing the field emission current itself. The ratio j_e/j_i at the cathode decreases with increasing voltage. It should be mentioned that while in macroscale gaps the ratio $j_e/j_i = \gamma_{se}$, in extremely small gaps the ratio $j_e/j_i \rightarrow \infty$ due to the absence of ionization. The $3\ \mu\text{m}$ gap is in the transition regime thereby leading to intermediate values of j_e/j_i at the cathode. Accurate prediction of parameters of such discharges requires a computational approach such as PIC/MCC simulations. The simulations were also used to estimate values of γ' , required in Eq. (3), using the relation⁴

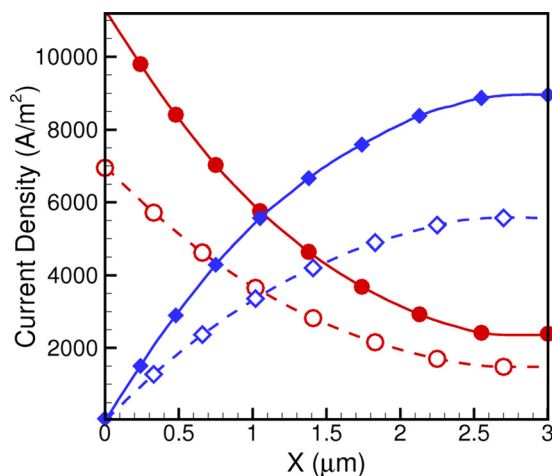


FIG. 3. (Color online) Comparison of ion and electron current density profiles across the $3\ \mu\text{m}$ nitrogen gap for an applied voltage of 153 V and 155 V. The solid lines with filled symbols correspond to 155 V and the dashed lines with open symbols correspond to 153 V. The diamond symbols correspond to ions and the circles correspond to electrons.

TABLE I. Summary of discharge parameters for a $3\ \mu\text{m}$ nitrogen gap for various applied voltages.

Voltage (V)	Q/Q_{150V}	j_{actual}/j_{FN}	$(j_e/j_i)_{\text{cathode}}$	$\gamma_{se} + \gamma'$	γ'
90	4.64×10^{-8}	3.0263	0.4921	0.0594	0.0094
120	0.0110	4.2105	0.3502	0.0960	0.0460
150	1.0000	5.8167	0.2721	0.1295	0.0795
153	1.9436	6.3714	0.2673	0.1454	0.0954
155	3.1034	7.0361	0.2614	0.1627	0.1127
157	5.2495	8.1748	0.2564	0.1866	0.1366

$$\gamma_{se} + \gamma' = \frac{1 - j_{FN} \exp(\alpha d) / j_{\text{actual}}}{\exp(\alpha d) - 1}, \quad (4)$$

which are also given in Table I. The value of γ' increases from being negligible at 90 V to about 0.15 at 157 V. It should be mentioned that γ' is a strong function of the ionization coefficient α which was obtained using Paschen curve parameters $A_p = 8.8$ and $B_p = 275$ for N_2 .⁴ The simulations predicted electron avalanche breakdown by the Townsend mechanism at a voltage of about 159 V for which the breakdown criterion in Eq. (3) would have to be satisfied indicating $\gamma' \approx 0.29$.

In summary, breakdown of gas in microgaps was studied using PIC/MCC simulations and observed directly by current measurements. The measured currents were described by Fowler-Nordheim theory using a value of field enhancement factor β that varies with voltage. The dynamic variation of β with voltage can be attributed to the erosion of surface impurities by the discharge leading to a decrease in β . PIC/MCC simulations of nitrogen microgaps showed that ionization of neutrals in the gap by field emitted electrons leads to a net positive charge that increases exponentially with applied voltage. For experimental conditions of $3\ \mu\text{m}$ gap, the combined effect of ionization in the gap and the resulting ion enhancement of field emission increases the current by factors of 5 and larger at 150 V and above leading to avalanche breakdown at 159 V. PIC/MCC simulations present a method of obtaining accurate mathematical models of the modified Paschen curve by quantifying functional dependence of the ion-enhancement on parameters such as the voltage, gap, gas composition, and field enhancement factor. The gas charging in micron-sized gaps, studied here for a DC bias, is expected to be more pronounced for voltage waveforms with polarity reversal due to effective increase in charge path length. Additionally, the effect of field emission would be enhanced for nanoscale gaps although there is a trade-off between the increased surface current density and the decreased ionization path length. These coupled effects can also be studied by the PIC/MCC technique used here.

The work has been supported by NNSA Center for Prediction of Reliability, Integrity and Survivability of Microsystems at Purdue University under Contract Number DE-FC52-08NA28617.

¹G. Rebeiz, *RF MEMS Theory, Design, Technology* (John Wiley & Sons, Inc., New York, 2003).

²D. Molinero, R. Comulada, and L. Castaner, *Appl. Phys. Lett.* **89**, 103506 (2006).

- ³G. Papaioannou, J. Papapolymerou, P. Pons, and R. Plana, *Appl. Phys. Lett.* **90**, 233507 (2007).
- ⁴Y. Raizer, *Gas Discharge Physics* (Springer, Berlin, 1991).
- ⁵D. Go and D. Pohlman, *J. Appl. Phys.* **107**, 103303 (2010).
- ⁶J. Torres and R. Dhariwal, *Nanotechnology* **10**, 102 (1999).
- ⁷A. Wallash and L. Levit, *Proc. SPIE* **4980**, 87 (2003).
- ⁸P. Czarnecki, X. Rottenberg, R. Puers, and I. D. Wolf, in *19th IEEE International Conference on MEMS*, Istanbul, Turkey (IEEE, Piscataway, NJ, 2006), pp. 890–893.
- ⁹J. Muldavin, C. Bozler, S. Rabe, P. Wyatt, and C. Keast, in 43rd Annual GOMAC Tech Conference, Orlando, FL, 16–19 March 2009.
- ¹⁰U. Zaghoul, B. Bhushan, P. Pons, G. Papaioannou, F. Coccetti, and R. Plana, *Nanotechnology* **22**, 035705 (2011).
- ¹¹R. Fowler and L. Nordheim, *Proc. R. Soc. London, Ser. A* **119**, 173 (1928).
- ¹²R. Burgess, H. Kroemer, and J. Houston, *Phys. Rev.* **90**, 515 (1953).
- ¹³T. Stern, B. Gossling, and R. Fowler, *Proc. R. Soc. London, Ser. A* **124**, 699 (1929).
- ¹⁴R. Tirumala and D. Go, *Appl. Phys. Lett.* **97**, 151502 (2010).
- ¹⁵A. Garg, A. Venkatraman, A. Kovacs, A. Alexeenko, and D. Peroulis, in *24th IEEE International Conference on MEMS*, Cancun, Mexico (IEEE, Piscataway, NJ, 2011), pp. 412–415.
- ¹⁶J. Verboncoeur, M. Alves, V. Vahedi, and C. K. Birdsall, *J. Comput. Phys.* **104**, 321 (1993).
- ¹⁷W. Zhang, T. Fisher, and S. Garimella, *J. Appl. Phys.* **96**, 6066 (2004).